

Supporting Information

Isoindole linkages provide a pathway for DOPAL-mediated crosslinking of α -synuclein

Jonathan W. Werner-Allen^a, Sarah Monti^b, Jenna F. DuMond^b, Rodney L. Levine^{b,*}, and Ad Bax^{a,*}

^aLaboratory of Chemical Physics, National Institute of Diabetes and Digestive and Kidney Diseases, and

^bLaboratory of Biochemistry, National Heart, Lung, and Blood Institute, National Institutes of Health, Bethesda, Maryland 20892, United States

*E-mail: rlevine@nih.gov, bax@nih.gov

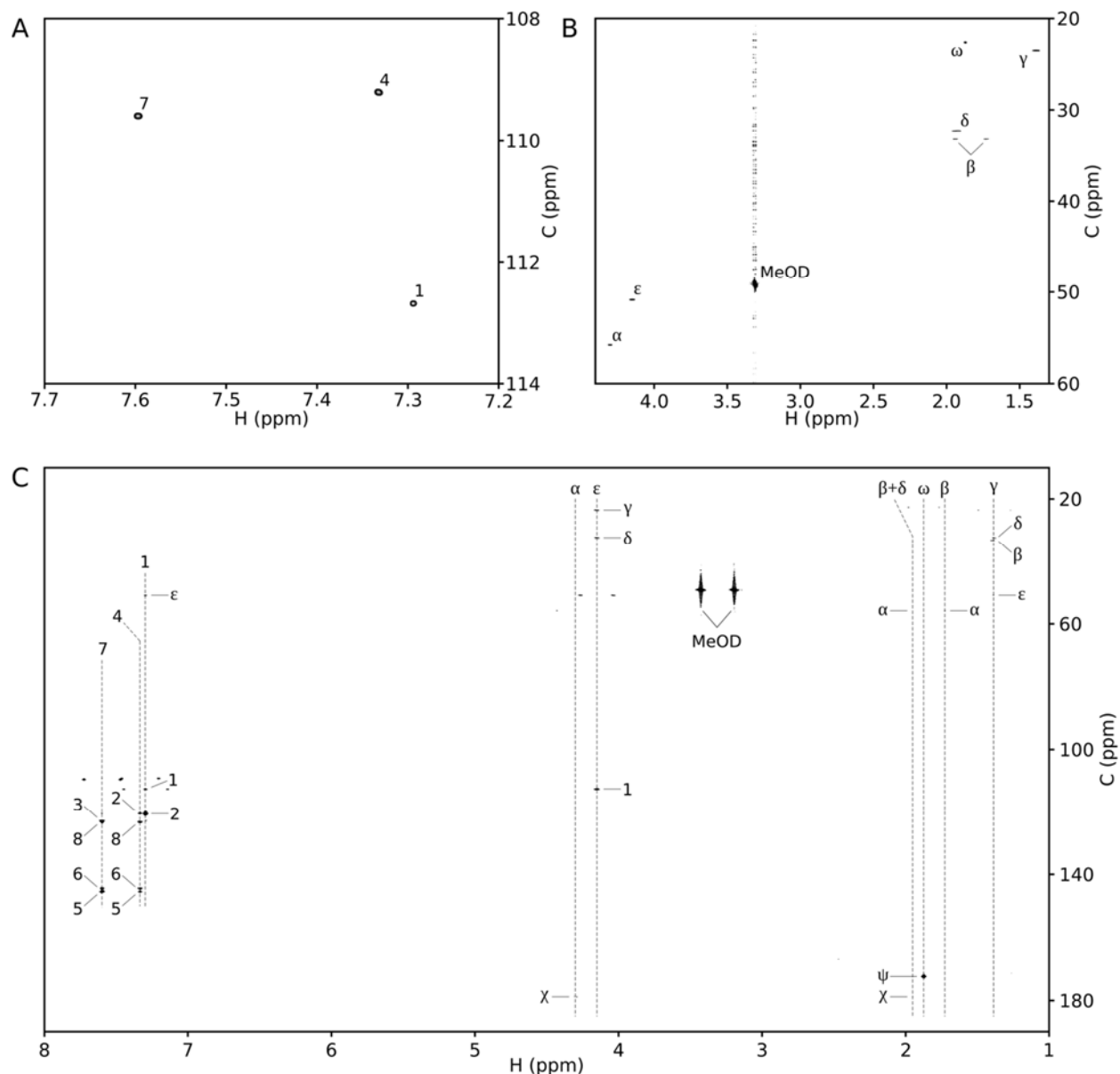


Figure S1. 2D ^1H - ^{13}C spectra for dicatechol isoindole lysine. **(A-B)** ^1H - ^{13}C HSQC spectra are shown for the aromatic (A) and aliphatic (B) resonances with labels corresponding to the annotated structure in Figure 3A. **(C)** The ring architecture of DCIL was elucidated with a ^1H - ^{13}C HMBC spectrum, which shares two defining characteristics with DCPL.¹ The first is a correlation between the terminus of the lysine sidechain (labeled ϵ) and the lone proton on the isoindole ring (labeled 1). Second, the isoindole proton (labeled 1) has a unique autocorrelation – at the position of a diagonal peak but without $^1\text{J}_{\text{HC}}$ splitting in the direct dimension – that results from the transfer of magnetization to its symmetric partner across the ring. The two remaining catechol protons (labeled 4 and 7) have correlations to both the hydroxyl-bearing positions (5 and 6) and to the carbon at the site of the new, intramolecular carbon-carbon bond that forms the isoindole ring (labeled 8).

Table S1. Chemical shifts for dicatchol isoindole lysine.

Dicatchol isoindole lysine		
	¹ H (ppm)	¹³ C (ppm)
ω	1.872	22.62
ψ		172.35
χ		178.83
α	4.300	55.78
β	1.734, 1.942	33.21
γ	1.390	23.50
δ	1.933	32.32
ε	4.149	50.85
1	7.293	112.73
2		120.57
3		122.83
4	7.332	109.24
5		145.56
6		144.47
7	7.596	109.63
8		123.24

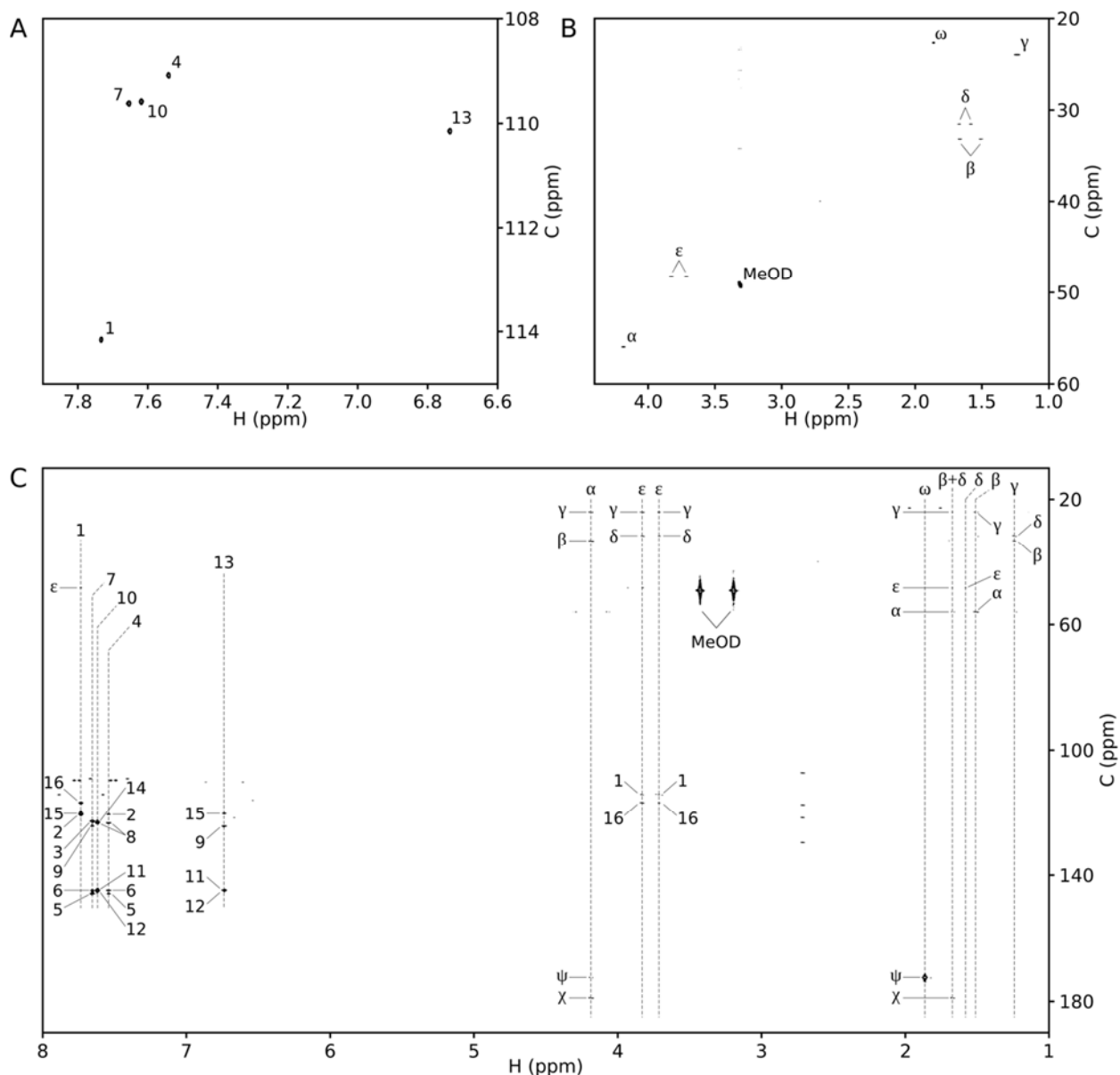


Figure S2. 2D ^1H - ^{13}C spectra for di-dicatechol isoindole lysine. **(A-B)** ^1H - ^{13}C HSQC spectra are shown for the aromatic (A) and aliphatic (B) resonances with labels corresponding to the annotated structure in Figure 4A. **(C)** The ^1H - ^{13}C HMBC spectrum for di-DCIL shares a similar pattern of correlations with the DCIL monomer. One notable difference arises because the di-DCIL intermolecular carbon-carbon bond breaks the symmetry of each isoindole ring, so that the sidechain terminus (labeled ϵ) is correlated to two nondegenerate carbon chemical shifts (labeled 1 and 16) rather than the single correlation observed for DCIL. The two halves of the di-DCIL dimer are symmetric, evidenced by the fact that its ten ring protons give only five aromatic signals. In (A-C), spectra are shown for a single isomeric form of di-DCIL (di-DCIL-1). The ^1H - ^{13}C HMBC correlations observed for the other isomer are identical.

Table S2. Chemical shifts for the two di-dicatechol isoindole lysine products.

	FP1		FP2		
	¹ H (ppm)	¹³ C (ppm)	¹ H (ppm)	¹³ C (ppm)	
ω	1.820	22.60	ω'	1.861	22.64
ψ		172.49	ψ'		172.38
χ		179.11	χ'		178.91
α	4.161	56.06	α'	4.185	55.94
β	1.323, 1.669	33.27	β'	1.512, 1.667	33.18
γ	1.252	24.30	γ'	1.240	23.95
δ	1.546	31.45	δ'	1.585, 1.671	31.54
ε	3.739, 3.844	48.56	ε'	3.714, 3.827	48.22
1	7.696	114.61	1'	7.732	114.17
2		120.36	2'		120.56
3		122.76	3'		122.75
4	7.527	109.09	4'	7.538	109.09
5		145.94	5'		145.93
6		144.88	6'		144.86
7	7.650	109.66	7'	7.651	109.63
8		123.31	8'		123.32
9		124.47	9'		124.35
10	7.616	109.66	10'	7.616	109.60
11		144.75	11'		144.73
12		144.77	12'		144.97
13	6.750	110.36	13'	6.733	110.16
14		123.10	14'		123.09
15		120.54	15'		120.26
16		116.69	16'		116.75

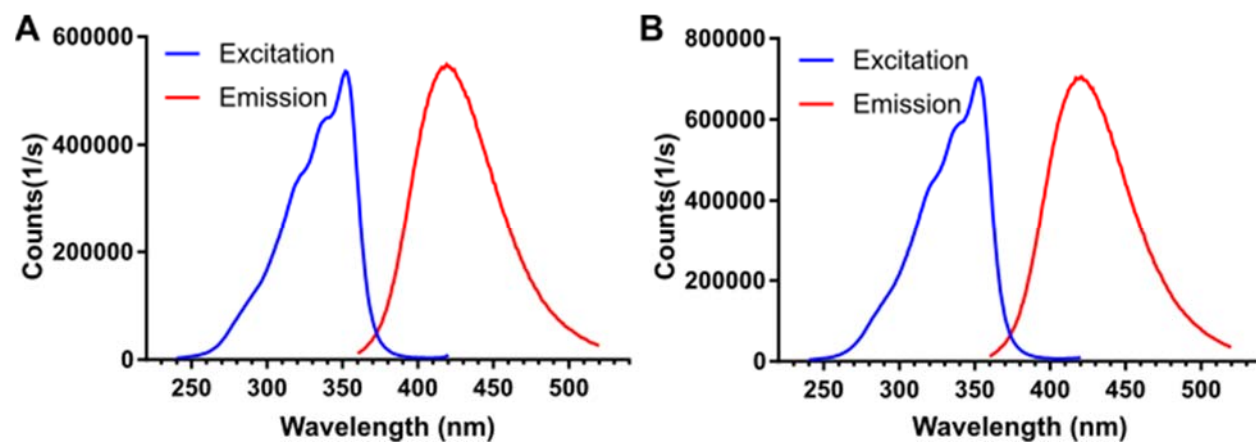


Figure S3. The di-dicatechol isoindole lysine compounds are fluorescent. Excitation and emission spectra for di-DCIL-1 (A) and di-DCIL-2 (B) show an excitation maximum at 357 nm and an emission maximum at 425 nm.

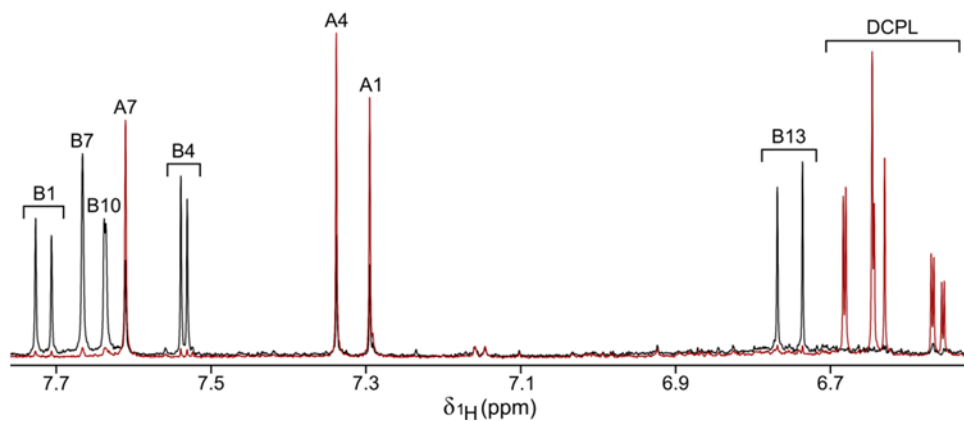


Figure S4. 1D ^1H NMR spectra of stable time point samples from the autoxidation of dicatechol pyrrole lysine confirm two successive products. Samples of $100\ \mu\text{M}$ DCPL in PBS with $100\ \mu\text{M}$ DTPA were incubated at $37\ ^\circ\text{C}$ for 7.5 minutes (red) or 67.5 minutes (black), flash frozen in liquid N_2 , lyophilized overnight, and resuspended in deuterated methanol. The spectra above show the aromatic region for the two samples. The first time point spectrum contains signals for the remaining DCPL and three singlets belonging to the initial degradation product, product A. In the second, there is residual product A along with five new singlets from a second product, product B. Like the acetyl methyl signals shown in Figure 2A, the aromatic signals of product B exist in pairs with very similar chemical shifts. Peak annotation for products A and B corresponds to the chemical structures in Figures 3A and 4A, respectively. Note that the line widths of the aromatic signals of products A and B are as narrow as DCPL in methanol, suggesting that the signal broadening observed in PBS (Figure 2C) is the result of a chemical exchange process that is unique to water.

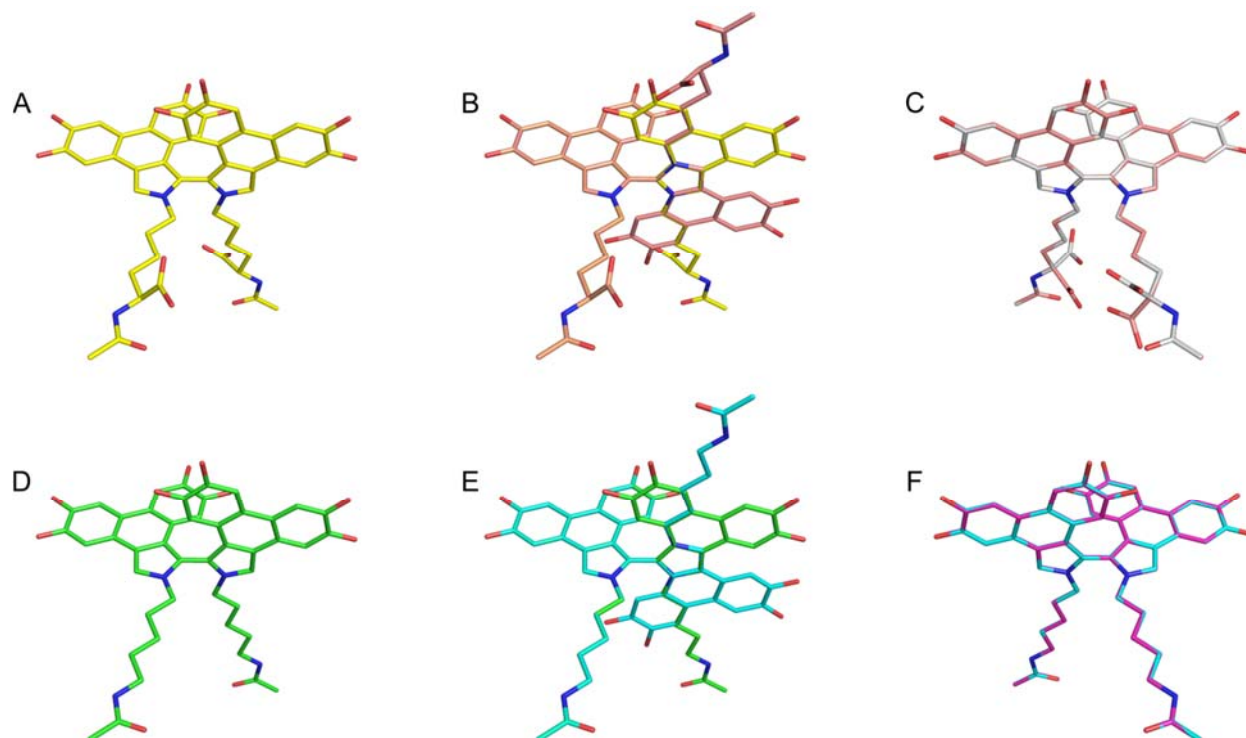


Figure S5. Di-dicatechol isoindole lysine atropisomers are chemically nonequivalent. **(A)** Three-dimensional structure of di-DCIL. Restricted rotation about the intermolecular carbon-carbon bond creates two stable atropisomers. In **(A)**, the intermolecular dihedral – defined by the nitrogens of the isoindole rings and the carbons of the intermolecular linkage is arbitrarily set to 90° . **(B)** The structure in **(A)** is overlaid with the second di-DCIL atropisomer (pink), with its intermolecular dihedral angle set to -90° , and aligned to the left-hand DCIL subunits. The orientations of the lysine sidechains and ring systems for the right-hand DCIL subunits are reversed in the two atropisomers. **(C)** The atropisomer of **(A)**, in pink, is aligned with the mirror image of **(A)**, in silver. While the orientation of the rings and lysine sidechains around the intermolecular bond is the same, the structures are not identical, as the atropisomer has inverted chirality (S configuration) at the lysine α carbon compared to the mirror image (R configuration). This difference would be expected to alter electrostatic interactions between the rings and the lysine carboxylates, and thus lead to disparities in the chemical shifts and chromatographic behavior for the two atropisomers. **(D)** Three-dimensional structure of di-dicatechol isoindole cadaverine. The intermolecular dihedral is set to 90° . **(E)** The structure in **(D)** is overlaid with its atropisomers (light blue). **(F)** In contrast to di-DCIL, the lack of chiral centers in di-DCIC means that the atropisomer of **(D)**, in light blue, and the mirror image of **(D)**, in purple, have identical structures, and thus the atropisomers of di-DCIC should be chemically equivalent and have identical chemical shifts.

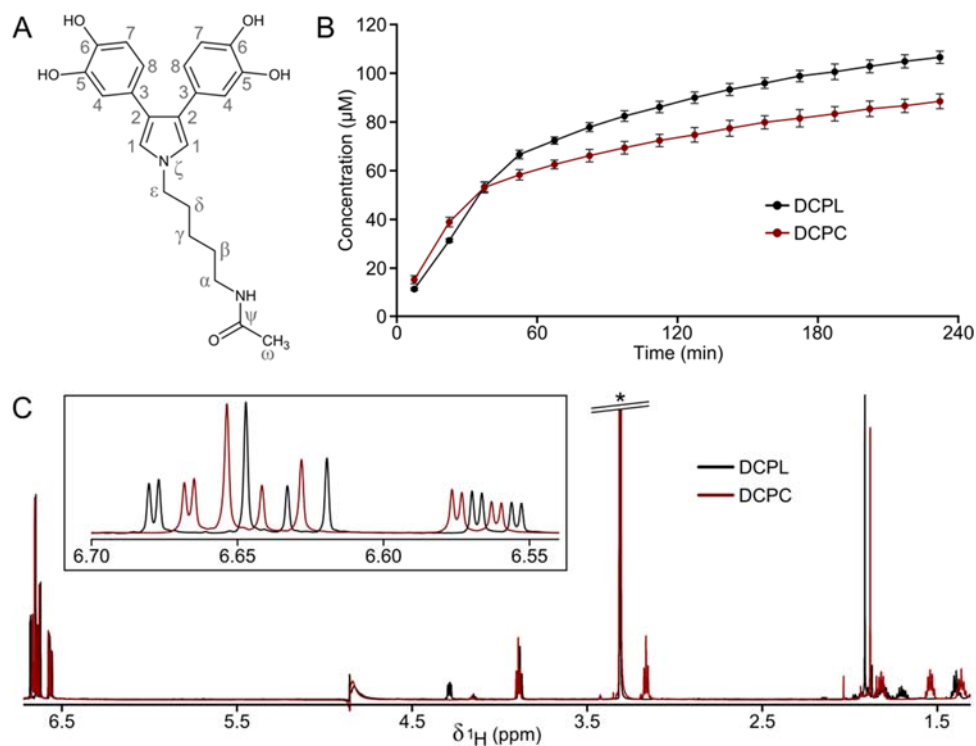


Figure S6. Formation of dicatechol pyrrole cadaverine. **(A)** Annotated structure of DCPC. The lack of a carboxyl group at the α position (as compared to DCPL) makes the molecule achiral. **(B)** The formation of dicatechol pyrrole compounds was followed in reactions in PBS at 37 °C with 2 mM DOPAL, 100 μM DTPA, 10% D_2O , and 2 mM of either Ac-Lys or Ac-cadaverine. The reactions were monitored using 1D ^1H NMR spectra and the concentrations of dicatechol pyrrole compounds were quantified by integration of the acetyl methyl signals as previously described.¹ Error bars represent standard deviations from three independent reactions. The rates and amounts of DCPL and DCPC production are similar. **(C)** Overlaid 1D ^1H NMR spectra of purified DCPL and DCPC in deuterated methanol. Residual solvent signal is marked with an asterisk. The inset is an expanded view of the aromatic region, containing the catechol signals and the characteristic pyrrolic singlets. Major deviations between the two compounds are centered at the α position as expected based on the difference in chemical structures, however, smaller deviations are also observed for the ring protons.

Table S3. Chemical shifts for dicatchol pyrrole cadaverine.

Dicatchol pyrrole cadaverine		
	¹ H (ppm)	¹³ C (ppm)
ω	1.882	22.38
ψ		173.11
α	3.163	40.14
β	1.538	29.75
γ	1.362	24.87
δ	1.818	32.03
ε	3.892	50.09
1	6.654	120.33
2		123.99
3		129.94
4	6.666	116.75
5		145.55
6		144.01
7	6.635	115.98
8	6.568	120.88

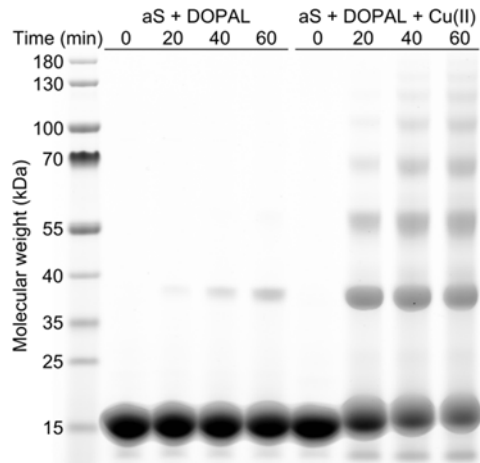


Figure S7. Cu(II) stimulates DOPAL-mediated crosslinking of α -synuclein. 100 μ M Ac-WT aS and 2 mM DOPAL were incubated at 37 $^{\circ}$ C in 100 mM MOPS pH 7.4 with or without 500 μ M CuCl₂. The reaction without CuCl₂ included 100 μ M DTPA to chelate any adventitious metals. Aliquots were taken over the course of an hour and subjected to SDS-PAGE. Cu(II) significantly accelerates the production of covalent synuclein oligomers, as previously reported by Jinsmaa *et al.*²

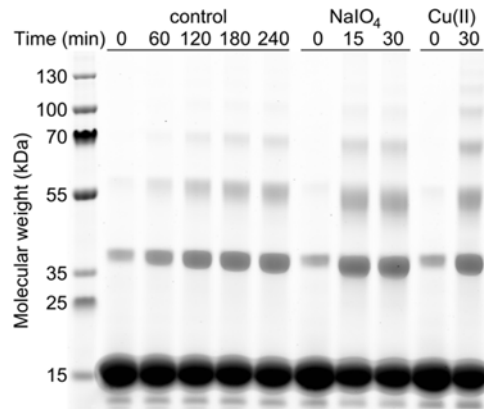


Figure S8. Oxidation drives crosslinking of DOPAL-reacted α -synuclein. Ac-WT aS was reacted with DOPAL for one hour to form adducts, then ethanol precipitated to remove unreacted DOPAL. Samples were resuspended at a concentration of 100 μ M DOPAL-reacted Ac-WT aS in either PBS with 100 μ M DTPA (control, NaIO₄) or 100 mM MOPS pH 7.4 without chelator (Cu(II)). Formation of α -synuclein oligomers was monitored by SDS-PAGE, with samples incubated at 37 °C for the indicated times. In the control reaction, no catalyst was added, and oligomers form relatively slowly over the course of a few hours. In the reactions labeled NaIO₄ and Cu(II), 500 μ M of sodium periodate or CuCl₂ were added, respectively, after the initial aliquot was withdrawn. Both compounds promote the rapid formation of crosslinks.

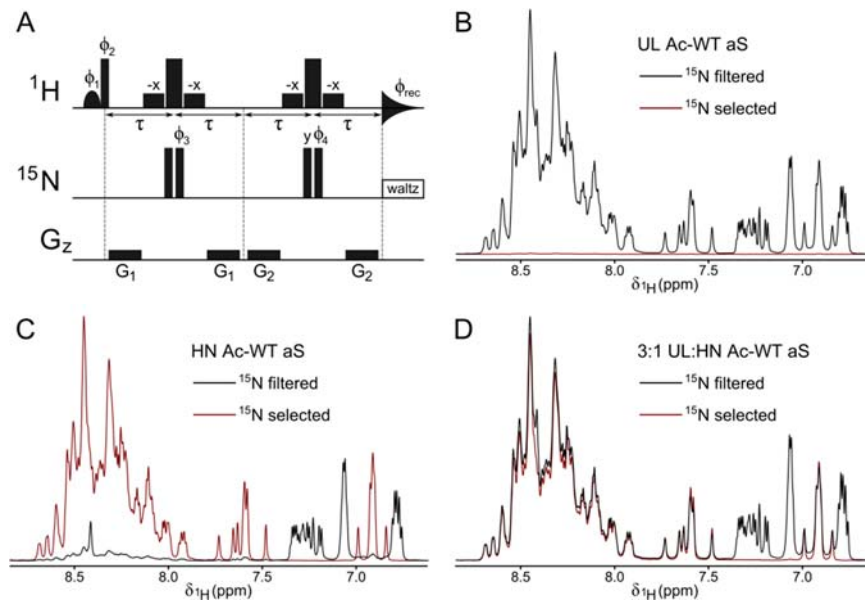


Figure S9. Measuring ^{15}N -labeled protein levels with 1D ^1H NMR spectra. **(A)** Pulse sequence for selection and filtering of ^{15}N -coupled ^1H signals. Narrow and wide bars indicate 90° and 180° pulses, respectively. The shaped bar represents a 1.5 ms, sinc shaped 90° water pulse. The short bars surrounding the 180° ^1H pulses are 1.2 ms rectangular pulses that function as WATERGATE sequences. All pulses are applied along x unless otherwise noted. The delay τ is 5.56 ms and gradients are rectangular shaped with durations and field strengths of $G_1 = (0.7 \text{ ms}, 11.9 \text{ G/cm})$ and $G_2 = (0.9 \text{ ms}, 7.7 \text{ G/cm})$. For ^{15}N filtering, phase cycling is $\phi_1 = [4(-x), 4x]$, $\phi_2 = [4x, 4(-x)]$, $\phi_3 = [x, -x]$, $\phi_4 = [2y, 2(-y)]$, and $\phi_{\text{rec}} = [4x, 4(-x)]$. For ^{15}N selection, the phase cycling is the same except for the receiver, which is set to $\phi_{\text{rec}} = [x, -x, -x, x, -x, x, x, -x]$. **(B-D)** Benchmarking of the ^{15}N -selection and -filtering 1D ^1H pulse sequence. In (B) and (C), the indicated spectra are collected with equal numbers of scans for samples of $100 \mu\text{M}$ Ac-WT aS that are either non-isotopically-labeled (B) or uniformly ^{15}N -labeled (C). In (C), the prominent signal in the amide region of the ^{15}N -filtered spectrum of ^{15}N -labeled Ac-WT aS is from the $\text{H}^{\text{c}1}$ proton on the imidazole ring of residue H50. In (D), the spectra are collected for a mixed sample containing $75 \mu\text{M}$ non-isotopically-labeled and $25 \mu\text{M}$ ^{15}N -labeled Ac-WT aS, and the ^{15}N -selected spectrum is collected with 3X the number of scans.

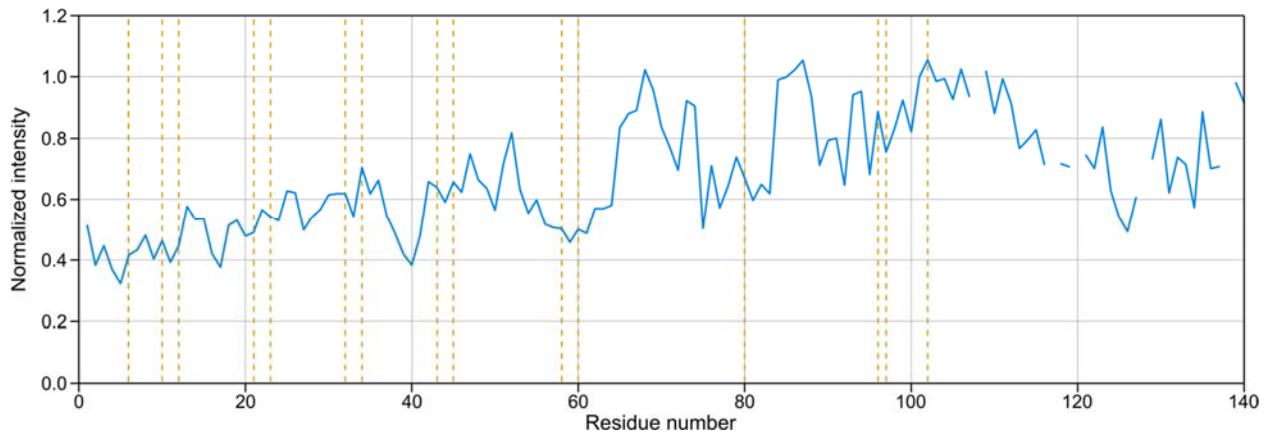


Figure S10. Crosslinking sites of dicatechol pyrrole lysine adducts to unmodified synuclein assessed by backbone amide ^1H - ^{15}N crosspeak intensity in 2D HSQC spectra. Non-isotopically-labeled, DOPAL-reacted Ac-WT aS was incubated with an equimolar amount of ^{15}N -labeled, unmodified Ac-WT aS to generate covalent oligomers. These were purified from the monomeric protein by size exclusion chromatography, and a ^1H - ^{15}N HSQC spectrum was collected to selectively probe modifications to the ^{15}N -labeled protein. The loss of native amide signal intensity reflects direct chemical modification at crosslinking sites as well as perturbations from altered transient intramolecular contacts and new intermolecular contacts in the oligomers. The positions of α -synuclein's 15 lysines are denoted by dashed orange lines. The signal intensity of each residue is normalized by its intensity in a spectrum of unmodified ^{15}N -labeled Ac-WT aS and the resulting intensity ratios were scaled so that residue G101, which appeared to be unaltered in the oligomer spectrum, is 1.0. Spectra of the oligomeric and unmodified Ac-WT aS samples are shown in Figure S10. The broad loss of native intensity for N-terminal residues mirrors that observed in reactions with DOPAL,¹ which targets α -synuclein's native lysines, but the attenuation of the C-terminus, which does not contain lysine, is more pronounced here.

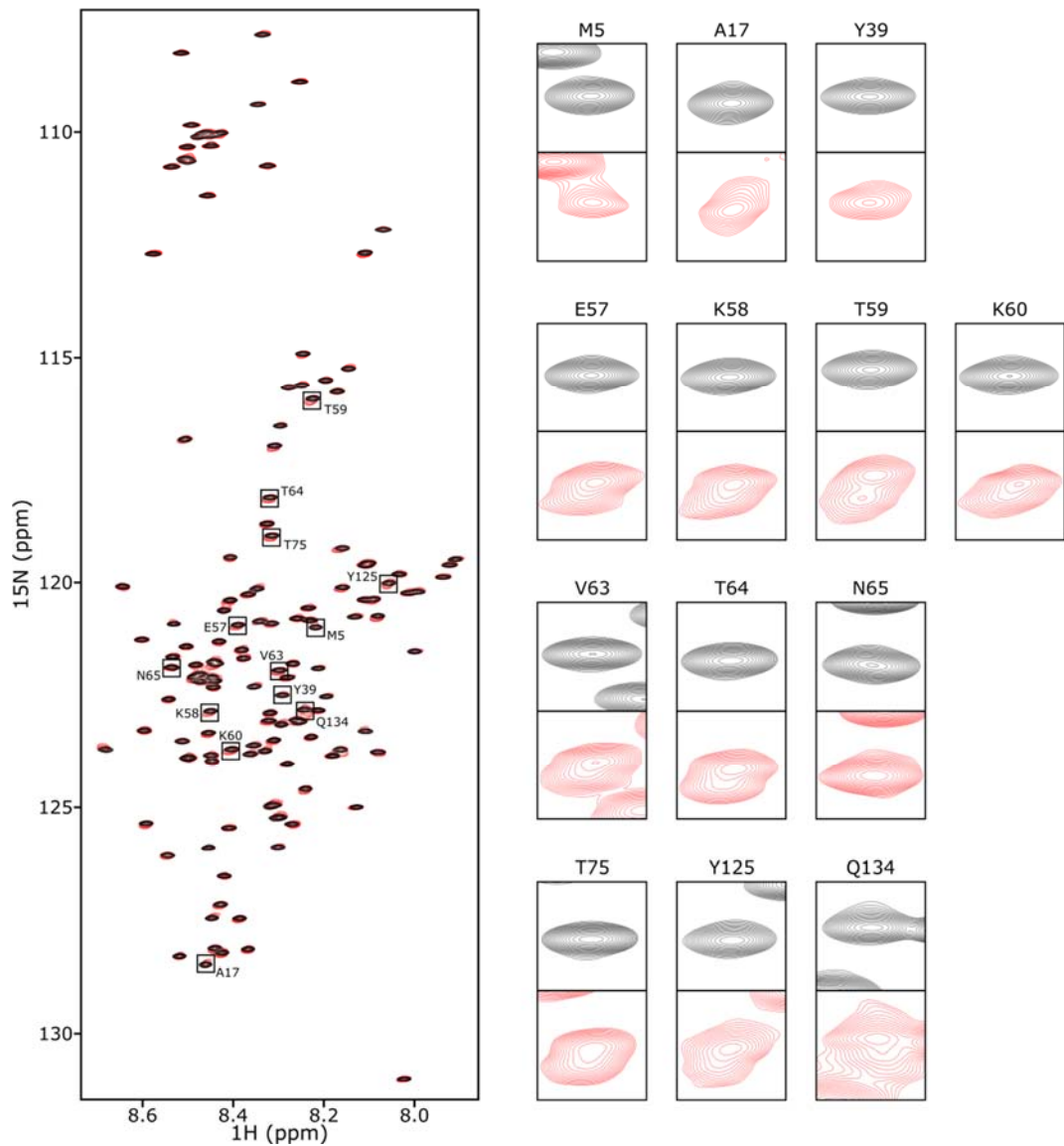


Figure S11. ^1H - ^{15}N HSQC spectra of unmodified and oligomer-incorporated Ac- αS . Spectra are plotted using exponential contours with a multiplication factor of 1.15. The black spectrum is from a control sample of unmodified, monomeric Ac- αS . The red spectrum is from $^1\text{H}/^{15}\text{N}$ -labeled Ac- αS in the oligomer sample analyzed in Figure 7 in the main text, and represents protein that was not directly modified by DOPAL, but incorporated into the oligomers by reacting with adducts on non-isotopically labeled protein in the second step of the crosslinking reaction. The left panel is an overlay of the two full spectra, and the panels on the right show individual amide signals with significant loss of native intensity in Figure S9. The second and third rows follow nondegenerate signals from the attenuated region starting at residue E57 until the return of near native intensity at residue N65. Native signal loss in the oligomeric sample has multiple causes. For some residues (e.g. M5 and Y39), intensity is lost but the residual signal appears relatively unaltered. Other residues (e.g. A17) exhibit heterogeneous line broadening similar to that observed in DOPAL-reacted samples.¹ In other cases (e.g. T59 and T64), a second discrete but nearly degenerate signal can be observed. This array of peak morphologies likely reflects the complexity of effects of DCPL-based crosslinking – including direct chemical modification at different linkage sites and potentially involving multiple residue types, altered

intramolecular transient interactions, and newly introduced intermolecular interactions in the oligomers – and is the focus of continuing study.

References

- [1] Werner-Allen, J. W., DuMond, J. F., Levine, R. L., and Bax, A. (2016) Toxic Dopamine Metabolite DOPAL Forms an Unexpected Dicatechol Pyrrole Adduct with Lysines of alpha-Synuclein, *Angew Chem Int Ed Engl* 55, 7374-7378.
- [2] Jinsmaa, Y., Sullivan, P., Gross, D., Cooney, A., Sharabi, Y., and Goldstein, D. S. (2014) Divalent metal ions enhance DOPAL-induced oligomerization of alpha-synuclein, *Neurosci Lett* 569, 27-32.